

Two boundary layers in Titan's lower troposphere inferred from a climate model

Benjamin Charnay* and Sébastien Lebonnois

Saturn's moon Titan has a dense atmosphere, but its thermal structure is poorly known. Conflicting information has been gathered on the nature, extent and evolution of Titan's planetary boundary layer—the layer of the atmosphere that is influenced by the surface—from radio-occultation observations by the Voyager 1 spacecraft¹ and the Cassini orbiter², measurements by the Huygens probe^{3–5} and by dune-spacing analyses⁶. Specifically, initial analyses of the Huygens data suggested a boundary layer of 300 m depth with no diurnal evolution⁴, incompatible with alternative estimates of 2–3 km (refs 1,2,6). Here we use a three-dimensional general circulation model⁷, albeit not explicitly simulating the methane cycle, to analyse the dynamics leading to the thermal profile of Titan's lowermost atmosphere. In our simulations, a convective boundary layer develops in the course of the day, rising to an altitude of 800 m. In addition, a seasonal boundary of 2 km depth is produced by the reversal of the Hadley cell at the equinox, with a dramatic impact on atmospheric circulation. We interpret fog that had been discovered at Titan's south pole earlier⁸ as boundary layer clouds. We conclude that Titan's troposphere is well structured, featuring two boundary layers that control wind patterns, dune spacing and cloud formation at low altitudes.

The planetary boundary layer (PBL) is the atmospheric layer located between the surface (land or sea), where friction slows down air motion, and the free atmosphere, where it becomes negligible⁹. The PBL is not restricted to Earth and should exist on any planet or moon with an atmosphere. The main differences between PBLs originate from their diurnal or seasonal evolution. On Earth, the height of the PBL (generally between 500 m and 3 km) is essentially controlled by solar heating and therefore by the diurnal cycle. A convective boundary layer appears during the morning when the ground is heated⁹, and the associated rise of warm air leads to the formation of cumuli that disappear in the evening. Because of its distance from the Sun and its thick and opaque atmosphere, Titan has a much weaker diurnal cycle than Earth (the insolation on Titan's surface is about 0.1% of that on Earth). The impact of this difference on the PBL has remained largely unexplored.

The thermal structure of Titan's lower troposphere (Titan's troposphere rises to 40 km) is difficult to measure. The first observations were obtained during the Voyager 1 flyby with two radio-occultation temperature profiles (at dawn and dusk). Both profiles gave a thermal lapse rate close to the dry adiabatic value (-1.31 K km^{-1}) below 3.5 km, followed by a slope change to -0.9 K km^{-1} above this altitude¹. It was concluded that the PBL should correspond to this 3.5 km layer. A more precise temperature profile was obtained by the Huygens probe during its descent³. The probe landed on Titan on 14 January 2005 at 9:47 am local true solar time. The landing site was located at $10.3^\circ \pm 0.4^\circ \text{ S}$, $167.7^\circ \pm 0.5^\circ \text{ E}$ in southern midsummer (solar longitude $L_s = 300.5^\circ$). It was possible

to derive the potential-temperature profile and the atmospheric composition there^{4,10}. The potential temperature decreased from 93.65 K at the ground to 93.48 K in the first 10 m and then remained approximately constant in the next 300 m. Above 300 m, the potential-temperature gradient becomes positive (Fig. 1a). An analytical calculation on the basis of these measurements led to the conclusion that this layer, interpreted as a convective layer, would not evolve by more than a few centimetres during Titan's day in this season⁴. In the thermal profile, a lapse-rate change at around 2 km altitude, together with a discontinuity at 800 m, has also been noticed, complicating the understanding of the PBL (ref. 5). Recent measurements by Cassini radio occultations² show adiabatic profiles up to 2 km for latitudes of around 30° S and a more stable profile at 53° S . Another piece of information on Titan's PBL can be derived from observations of its giant linear dunes in the equatorial band (Titan has the largest dune fields in the Solar System)¹¹. The formation of giant dunes is a complex phenomenon depending on both surface winds and the PBL. The latter controls the height of the dunes and the spacing by promoting the growth of dunes with wavelength of the order of magnitude of the PBL height¹². Thus, observation of dune spacing of around 3 km suggests the presence of a PBL 2–3 km thick⁶.

To clarify the situation concerning Titan's PBL and its evolution during the diurnal cycle, we used a three-dimensional general circulation model (GCM; Methods). As the radiative time constant in Titan's troposphere is larger than 2.5 Titan years¹³, direct solar heating of the troposphere is unable to generate a diurnal or even seasonal cycle. However, solar heating of the surface can induce diurnal variations in the lower troposphere through the sensible heat flux. The temperature lapse-rate profile simulated by the GCM for the Huygens site at the time of landing is in agreement with the measured profile and features three particular levels, denoted A, B and C (Fig. 1b).

Level A corresponds to the top of a convective boundary layer (also called the mixed layer) developed at 10 am by ground heating. For the Huygens landing site, the solar flux at the top of the atmosphere reaches a maximum of 15 W m^{-2} with a diurnal average value of 4.8 W m^{-2} , 10% of which reaches the surface. The modelled ground temperature varies by 0.4 K over one Titan day (Supplementary Fig. S1), so less than Cassini Composite Infrared Spectrometer observations¹⁴ (1–1.5 K). The sensible flux at ground level varies from -0.05 W m^{-2} in the night to $+1.1 \text{ W m}^{-2}$ at midday (Supplementary Fig. S1), with an average value of $+0.23 \text{ W m}^{-2}$. This represents approximately 5% of the solar flux at the top of the atmosphere and around 60% of the solar flux absorbed by the surface. The modelled wind is about 0.3 m s^{-1} at 30 m. In the convective layer, the temperature profile follows the adiabatic lapse rate. According to our simulations, dry convection starts after 7 am local true solar time in the southern hemisphere (Fig. 2). Then, the convective boundary layer rises, reaching a

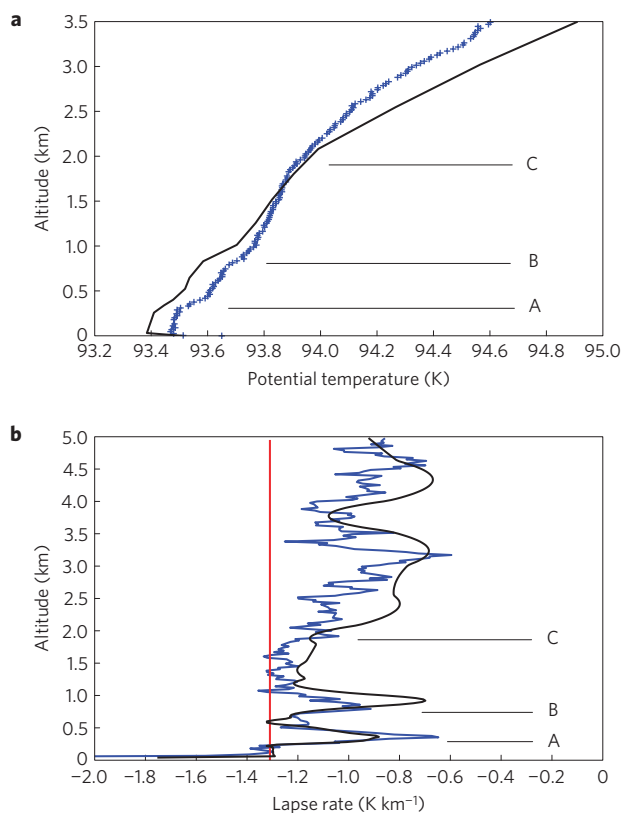


Figure 1 | Thermal structure of the first kilometres at the Huygens landing site, measured by the Huygens Atmospheric Structure Instrument and simulated by the GCM. a, Potential temperature observed during the Huygens probe descent (blue crosses; the temperature uncertainty is ± 0.25 K) and simulated with our GCM (black line). **b**, Temperature lapse rate observed during the Huygens probe descent (blue) and simulated with our GCM (black). The red line indicates the adiabatic lapse rate. Note that the model faithfully predicts the major features in the thermal structure (levels A, B and C). The characteristic peaks A and B are related to the diurnal evolution of the PBL, whereas the slope change C is related to the seasonal evolution of the PBL.

maximal altitude of approximately 800 m at 3 pm, and disappears after 5 pm. After sunset, the air cools close to the ground, producing a stable 100 m layer (observed in the Cassini radio-occultation dawn profiles²). Owing to low turbulent heat diffusion and strong atmospheric stability, the structure at 800 m (called the residual layer, level B) remains observable throughout the day, with the temperature lapse rate slightly below the adiabatic value. A similar layer has been observed at 900 m in one of the Cassini radio-occultation profiles².

Above 1 km and up to 2 km (level C), the thermal profile of the troposphere is again close to the adiabatic lapse rate. This involves a physical process different from the diurnal boundary layer (limited to the first 800 m) mixing the air at this height. We explain this phenomenon by the seasonal cycle^{15,16} producing a seasonal boundary layer. For most of the time, Titan's circulation is controlled by a pole-to-pole Hadley cell. The circulation of this cell reverses at the equinox, but this transition is not instantaneous: the intertropical convergence zone (ITCZ, where the air rises) runs through all latitudes from one pole to the other, with the formation of two Hadley cells during the transition¹⁷. Thus, twice a Titan year, the ITCZ crosses the equatorial band and warm air rises to the free atmosphere at 2 km. The potential temperature in the free atmosphere shows little seasonal or latitudinal variation and follows a linear profile. The 2 km height is then fixed by the

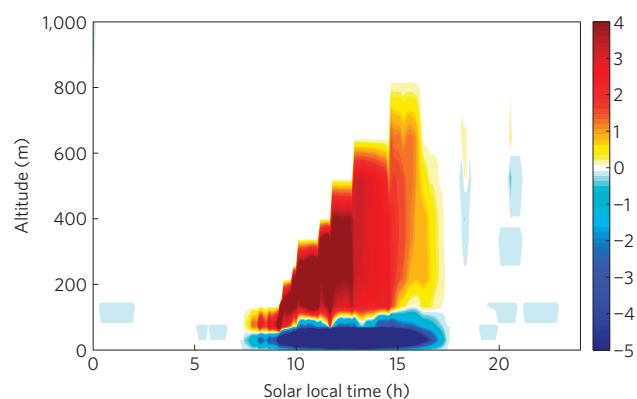


Figure 2 | Simulated diurnal evolution of dry convection in the first kilometre during one typical Titan day at the Huygens site. Temperature tendencies (in 10^{-7} K s^{-1}) due to dry convection, illustrating the vertical extension of the convective layer during one typical Titan day at the Huygens probe landing site and season. The steps in the figure are caused by the vertical discretization of our model.

constant lapse rate in the free atmosphere (around -0.8 K km^{-1}) and the ground temperature (Fig. 3). The layer remains as a residual layer after the passage of the ITCZ. For example, the layer at the Huygens site was produced ten terrestrial years before the landing. Moreover, sporadic convection is maintained, owing to global circulation. In our simulation, the slope change at 2 km has a dramatic consequence for meridional circulation. It acts as a cap layer, blocking most of the vertical rising (weak on Titan). Therefore most of the meridional circulation is confined to the first 2 km, leading to heating and convection in this layer at all latitudes covered by this circulation. The seasonal cycle enforces a higher stability in winter (Fig. 3) or at high latitude, except for the summer solstice, as observed². This trapped Hadley circulation controls winds in the lower troposphere. Zonal winds in the first 2.5 km of the Huygens profile¹⁸ correspond to summer monsoon winds (Supplementary Fig. S2). The free atmosphere begins above this level: the temperature, controlled by direct solar heating, is maximal at the equator, causing an increase of zonal winds with altitude. In conclusion, although Titan's Hadley circulation reaches the tropopause and above, its strength is mainly confined to the first 2 km. The thermal structure is thus based on two boundary layers: a diurnal layer produced by ground heating and a seasonal layer produced by the ITCZ displacement at the equinox, weaker the rest of the year, but maintained by the global circulation.

Averaged over more than one day, only a weak PBL signature remains at level B. The slope change (level C) becomes the largest significant feature in the thermal structure (Fig. 3). In this respect, it is equivalent to a permanent boundary layer of around 2 km for all in the equatorial band (30° S – 30° N). Interfacial waves can appear on the top of this layer, controlling giant dune size¹². The height of 2 km is consistent with the observed dune spacing of 3 km (ref. 6). Furthermore, at these latitudes, this layer is particularly marked at the equinox, in agreement with a scenario proposed for the preferential formation of the dunes during this period¹⁹.

As our model does not take into account clouds and the methane cycle, all results correspond to a dry case. Episodic deep convection can happen^{20,21} when the atmosphere is saturated. In such a case, its lapse rate is reajusted to the moist adiabatic lapse rate (around -0.6 K km^{-1} ; refs 5,17). Such events might leave footprints in the thermal profile, but they remain rare. Furthermore deep convection is expected to be mainly restricted to the middle troposphere⁵. Over an area of liquid methane (for

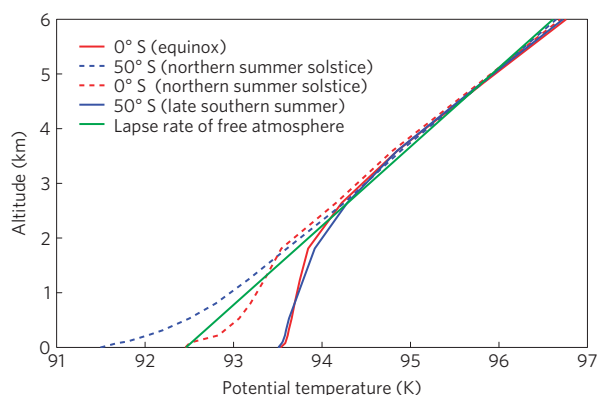


Figure 3 | Simulated averaged potential-temperature profiles giving the seasonal evolution of the thermal structure for the first kilometres.

Averaged potential-temperature profile over ten Titan days for different latitudes (red at the equator, blue at 50° S) and at different seasons: solid line at the ITCZ crossing (equinox for the equator and late southern summer for 50° S) and dashed line in the coldest period (northern summer solstice for both). The green line corresponds to the lapse rate of the free atmosphere (above 2 km).

example the polar lakes), methane evaporation and the associated latent flux will strongly modify the development of the diurnal PBL. However, for lands with limited moisture at the ground (this includes areas surrounding lakes), the diurnal PBL should remain close to the dry case.

Clouds are observed in Titan's middle or higher troposphere. Most of them are produced by large-scale ascending motion of methane to altitudes where the air is saturated^{22–24}. Clouds have also been detected at 750 m, below the usual altitude of tropospheric clouds (higher than 10 km). They have been interpreted as fog formed above the ground in high-humidity conditions⁸, but have not yet been explained, diurnal temperature variations being too limited to generate fog by cooling. In our simulations, the top of the diurnal PBL reaches 700–800 m for all summer latitudes (5° S–80° S, except at the ITCZ, where it rises to 2 km), precisely the altitude of the fog. Therefore, we propose this fog corresponds to boundary-layer clouds, produced by the same mechanism as fair-weather cumuli on Earth. During summer in polar regions (where lakes and pools of methane are present), humidity close to the ground may reach high values. In the morning, dry convection is triggered and methane-rich air close to the ground rises to the top of the PBL. For an air parcel close to saturation near the ground that rises to 750 m, the relative humidity can increase by up to 8%, which is sufficient to trigger condensation. These clouds could appear during the morning at high latitudes in summer, but also after precipitation in other regions^{20,21}, in particular at the ITCZ, where they could form up to 2 km. Mesoscale simulations, including cloud-formation schemes, will be required to fully validate our conclusions.

Our simulations provide a general framework that explains a number of different meteorological observations and features on Titan. They reveal that, despite the limited solar insolation, the diurnal cycle on Titan is an active and observable phenomenon. In this matter, Titan therefore seems closer to an Earth-like world than previously anticipated⁴.

Methods

For this study, we used a three-dimensional GCM (ref. 7) derived from the first Titan GCM developed by our team²⁵, but benefiting from the most up-to-date dynamical core²⁶. It covers altitudes from the surface to 500 km. It includes the McKay radiative code²⁷ with diurnal cycle, fully coupled aerosol microphysics²⁸, a Mellor–Yamada boundary-layer scheme²⁹ and gravitational tides⁴ but no methane cycle. We simply used a methane profile close to that observed by

Huygens for the radiative transfer. Our model produces superrotation in the stratosphere with a winter jet of 120 m s⁻¹, slightly below the observed values^{25,28,30}. Tropopause temperature is close to 70 K and the zonal wind profile from the surface to 140 km closely follows the profile retrieved from the Huygens probe, including a minimum in the 60–80 km region. Simulations were carried out with a 32 × 48 longitude–latitude horizontal resolution and 73 vertical levels (35 in the troposphere). The first level is at 30 m. Physical constants used for the surface were albedo = 0.15, thermal inertia = 400 J m⁻² K⁻¹ s^{-1/2}, emissivity = 0.95 and rugosity = 0.005 m. We verified that the development of the PBL occurs for any realistic values of these constants. Further details are given in Supplementary Information.

Received 5 August 2011; accepted 16 December 2011;
published online 15 January 2012

References

- Lindal, G. F. *et al.* The atmosphere of Titan: An analysis of the Voyager 1 radio occultation measurements. *Icarus* **53**, 348–363 (1983).
- Schinder, P. J. *et al.* The structure of Titan's atmosphere from Cassini radio occultations. *Icarus* **215**, 460–474 (2011).
- Fulchignoni, M. *et al.* *In situ* measurements of the physical characteristics of Titan's environment. *Nature* **438**, 1–7 (2005).
- Tokano, T., Ferri, F., Colombatti, G., Mäkinen, T. & Fulchignoni, M. Titan's planetary boundary layer structure at the Huygens landing site. *J. Geophys. Res.* **111**, E08007 (2006).
- Griffith, C. A., McKay, C. P. & Ferri, F. Titan's tropical storms in an evolving atmosphere. *Astrophys. J. Lett.* **687**, L41–L44 (2008).
- Lorenz, R. D., Claudin, P., Andreotti, B., Radebaugh, J. & Tokano, T. A 3 km atmospheric boundary layer on Titan indicated by dune spacing and Huygens data. *Icarus* **205**, 719–721 (2010).
- Lebonnois, S., Burgalat, J., Rannou, P. & Charnay, B. Titan Global Climate Model: A new 3-dimensional version of the IPSL Titan GCM. *Icarus* <http://dx.doi.org/10.1016/j.icarus.2011.11.032> (2011).
- Brown, M. E., Smith, A. L., Chen, C. & Ádámkóvics, M. Discovery of fog at the South Pole of Titan. *Astrophys. J. Lett.* **706**, L110–L113 (2009).
- Parlange, M. B., Eichinger, W. E. & Albertson, J. D. Regional scale evaporation and the atmospheric boundary layer. *Rev. Geophys.* **33**, 99–124 (1995).
- Niemann, H. B. *et al.* The abundances of constituents of Titan's atmosphere from the GCMS instrument on the Huygens probe. *Nature* **438**, 1–6 (2005).
- Lorenz, R. D. *et al.* The sand seas of Titan: Cassini RADAR observations of longitudinal dunes. *Science* **312**, 724–727 (2006).
- Andreotti, B., Fourriere, A., Ould-Kaddour, F., Murray, B. & Claudin, P. Size of giant aeolian dunes limited by the average depth of the atmospheric boundary layer. *Nature* **457**, 1120–1123 (2009).
- Tokano, T., Neubauer, F. M., Laube, M. & McKay, C. P. Seasonal variation of Titan's atmospheric structure simulated by a general circulation model. *Planet. Space Sci.* **47**, 493–520 (1999).
- Cottini, V. *et al.* Spatial and temporal variations in Titan's surface temperatures from Cassini CIRS observations. *Planet. Space Sci.* <http://dx.doi.org/10.1016/j.pss.2011.03.015> (2011).
- Jennings, D. E. *et al.* Titan's hydrogen torus. *Astrophys. J.* **246**, 344–353 (1981).
- Friedson, A. J., West, R. A., Wilson, E. H., Oyafuso, F. & Orton, G. S. A global climate model of Titan's atmosphere and surface. *Planet. Space Sci.* **57**, 1931–1949 (2009).
- Mitchell, J. L. The drying of Titan's dunes: Titan's methane hydrology and its impact on atmospheric circulation. *J. Geophys. Res.* **113**, E08015 (2008).
- Tokano, T. The dynamics of Titan's troposphere. *Phil. Trans. R. Soc. A* **367**, 633–648 (2009).
- Tokano, T. Relevance of fast westerlies at equinox for eastward elongation of Titan's dunes. *Aeolian Res.* **2**, 113–127 (2010).
- Turtle, E. P. *et al.* Rapid and extensive surface changes near Titan's equator: Evidence of April showers. *Science* **331**, 1414–1417 (2011).
- Mitchell, J. L., Adamkóvics, M., Caballero, R. & Turtle, E. P. The impact of methane thermodynamics on seasonal convection and circulation in a model Titan atmosphere. *Nature Geosci.* **4**, 589–592 (2011).
- Rodríguez, S. *et al.* Global circulation as the main source of cloud activity on Titan. *Nature* **459**, 678–682 (2009).
- Rannou, P., Montmessin, F., Hourdin, F. & Lebonnois, S. The latitudinal distribution of clouds on Titan. *Science* **311**, 201–205 (2006).
- Mitchell, J. L., Pierrehumbert, R. T., Frierson, D. & Caballero, R. The dynamics behind Titan's methane cloud. *Proc. Natl Acad. Sci. USA* **103**, 18421–18426 (2006).
- Hourdin, F. *et al.* Numerical simulation of the general circulation of the atmosphere of Titan. *Icarus* **117**, 358–374 (1995).

26. Hourdin, F. *et al.* The LMDZ4 general circulation model: Climate performance and sensitivity to parameterized physics with emphasis on tropical convection. *Clim. Dynam.* **27**, 787–813 (2006).
27. McKay, C. P., Pollack, J. B. & Courtin, R. The thermal structure of Titan's atmosphere. *Icarus* **80**, 23–53 (1989).
28. Rannou, P., Hourdin, F., McKay, C. P. & Luz, D. A coupled dynamics–microphysics model of Titan's atmosphere. *Icarus* **170**, 443–462 (2004).
29. Hourdin, F., Couvreux, F. & Menut, L. Parameterization of the dry convective boundary layer based on a mass flux representation of thermals. *J. Atmos. Sci.* **59**, 1105–1123 (2002).
30. Crespin, A. *et al.* Diagnostics of Titan's stratospheric dynamics using Cassini/CIRS data and the IPSL General Circulation Model. *Icarus* **197**, 556–571 (2008).

Acknowledgements

We are grateful to F. Forget and R. Wordworth for advice and corrections to the paper. We thank N. Rochetin for discussions of the terrestrial climate. This study was supported by an Agence Nationale de la Recherche grant.

Author contributions

S.L. and B.C. developed this version of the model. B.C. ran and analysed simulations. B.C. and S.L. wrote the manuscript.

Additional information

The authors declare no competing financial interests. Supplementary information accompanies this paper on www.nature.com/naturegeoscience. Reprints and permissions information is available online at <http://www.nature.com/reprints>. Correspondence and requests for materials should be addressed to B.C.

Two boundary layers in Titan's lower troposphere inferred from a climate model Supplementary information

Benjamin Charnay and Sébastien Lebonnois

1 Description of the IPSL Titan GCM

For this study, we used a 3-dimensional GCM¹ derived from the first Titan GCM developed by our team². It covers altitudes from the surface to 500 km. The initial state was taken from our 2-dimensional studies³ and the simulation was run for 12 years, with a seasonal cycle satisfyingly stable. Our model produces superrotation in the stratosphere with a winter jet of 120 m/s slightly below the observed values²⁻⁴. Tropopause temperature is close to 70 K and the zonal wind profile from the surface to 140 km closely follows the profile retrieved from the Huygens probe, including a minimum in the 60-80 km region. The question of the development of super-rotation from a resting state remains to be studied in more details, as discussed in a subsequent work¹.

- *dynamical core*: based on the most up-to-date version of the LMDZ⁵. This dynamical core is based on a finite-difference discretization scheme that conserves both potential enstrophy for barotropic nondivergent flows, and total angular momentum for axisymmetric flows. A longitudinal filter is applied in the polar regions (poleward of 60° latitude) to limit the effective resolution to that at 60°. The version used in this study includes gravitational tides⁶, though the impact in the

troposphere do not influence the effects described in this work. We found tidal effects on the pressure similar to previous works^{6,7}, but tidal winds are far much weaker with our model.

- *microphysics*: fully coupled aerosol microphysics calculated in 2D (zonally averaged)⁴.
- *methane cycle*: the present model is dry and does not taken into account the methane cycle. The profile of methane is fixed (close to the HASI profile⁸) for the radiative transfert
- *radiative code*: based on the McKay radiative code⁹ and including diurnal cycle.
- *boundary layer*: based on the Mellor-Yamada boundary layer scheme^{10,11}

Grid parameters and radiative time step:

- *Horizontal resolution*= 32x48
- *Vertical resolution*= 73 levels (35 in the troposphere)
- *Altitude of the first level*= 30 m
- *Call of the radiative transfert*= 200/ Titan day

Physical constants used for the surface:

- *Albedo*= 0.15
- *Thermal inertia*= 400 J m⁻² K⁻¹
- *Emissivity*= 0.95
- *Surface rugosity*= 0.005 m

2 Diurnal cycle at the Huygens' site

At the Huygens' site, the model gives surface temperature variations of around 0.4 K over one typical Titan day (Figure S1 a). The diurnal variations of the different fluxes (solar heating, infrared cooling and sensible flux) are represented in Figure S1 b. During the day, around 60% of the solar flux absorbed by the surface is converted into sensible flux. At the Huygens' site, the sensible flux represents around 5% of the solar insolation at the top of the atmosphere. Averaged over all Titan, it represents 4% of the solar insolation, a value four times higher than in the 1D McKay model¹².

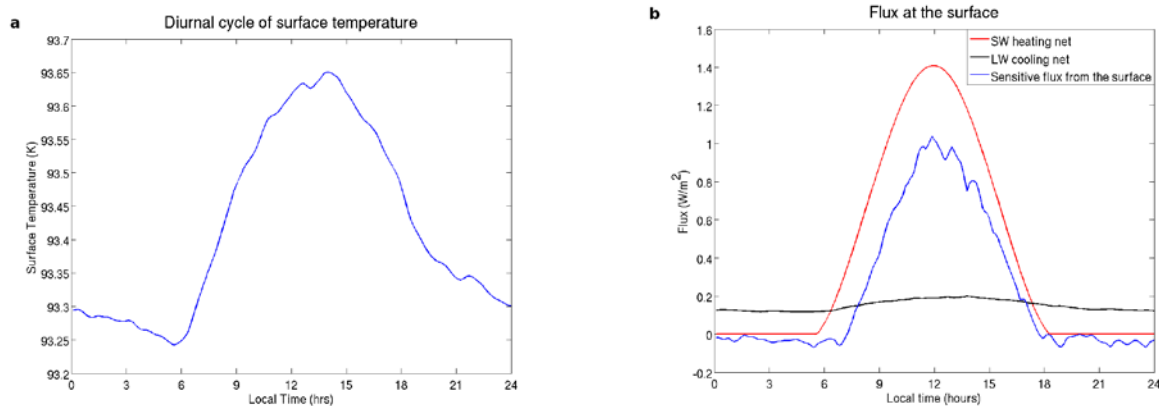


Figure 1: **Effect of the diurnal cycle on temperature and flux budget at the surface.** **a**, Diurnal surface temperature variation during one typical day at the Huygens' site. **b**, Diurnal variation of fluxes at the surface at the Huygens' site. The shortwave solar heating (in red), the infrared cooling (in black) and the sensible flux from surface to atmosphere (in blue) are shown.

3 Winds at the Huygens' site

Figure S2 corresponds to the wind profiles for the first kilometers, derived from the Huygens probe¹³ and produced by the GCM. The GCM winds have been averaged over one Titan day. The simulated wind profile shows the same tendencies as the observed one. We can interpret these tendencies thanks to the two boundary layers: increase of the wind intensity in the first few hundred meters (caused by the surface friction of the diurnal boundary layer) and control of its orientation in the first 2 km by the trapped Hadley cell. The dominant simulated meridional circulation is trapped in the first two kilometers. The Huygens' profile does not show a weakening of meridional wind above 2 km, but it corresponds to an instantaneous profile where waves and topographic effects may have an effect. Winds (simulated and observed) in the 2.5 first km correspond to summer moonson winds¹⁴. The zonal wind is prograde close to the surface and become retrograde above 700 m. Then it increases above 2.5 km (free atmosphere with the latitudinal temperature gradient oriented toward the equator).

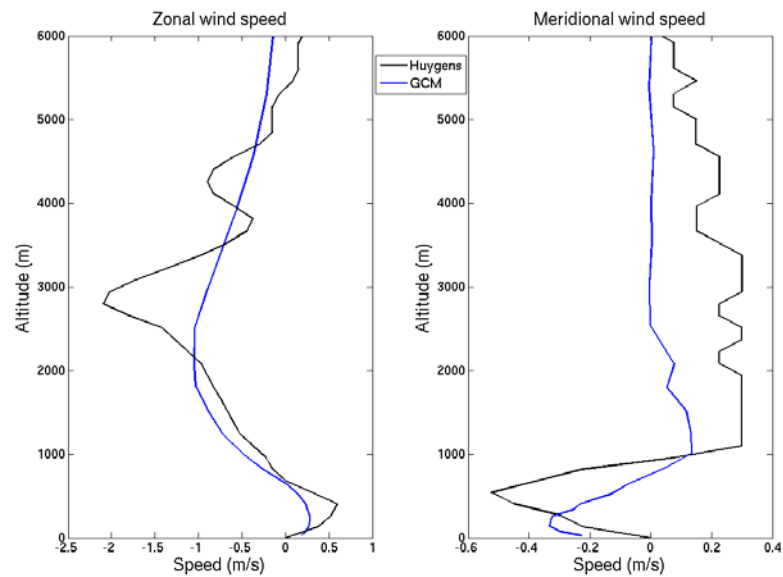


Figure 2: Averaged zonal and meridional winds for the first kilometers at the Huygens site. On the left: zonal wind, on the right: meridional wind. In blue: wind profiles from the GCM, averaged over one day. In black: instantaneous wind profiles derived from the Huygens probe¹³.

References

1. Lebonnois, S., Burgalat, J., Rannou, P. & Charnay, B. Titan Global Climate Model: a new 3-dimensional version of the IPSL Titan GCM. *Icarus* (2011).
2. Hourdin, F. *et al.* Numerical simulation of the general circulation of the atmosphere of Titan. *Icarus* **117**, 358–374 (1995).

3. Crespin, A. *et al.* Diagnostics of Titan's stratospheric dynamics using Cassini/CIRS data and the IPSL General Circulation Model. *Icarus* **197**, 556–571 (2008).
4. Rannou, P., Hourdin, F., McKay, C. P. & Luz, D. A coupled dynamics-microphysics model of Titan's atmosphere. *Icarus* **170**, 443–462 (2004).
5. Hourdin, F. *et al.* The LMDZ4 general circulation model: climate performance and sensitivity to parameterized physics with emphasis on tropical convection. *Clim. Dyn.* **27**, 787–813 (2006).
6. Tokano, T., Ferri, F., Colombatti, G., Mäkinen, T. & Fulchignoni, M. Titan's planetary boundary layer structure at the Huygens landing site. *J. Geophys. Res.* **111**, 8007 (2006).
7. Friedson, A. J., West, R. A., Wilson, E. H., Oyafuso, F. & Orton, G. S. A global climate model of Titan's atmosphere and surface. *Planet. & Space Sci.* **57**, 1931–1949 (2009).
8. Niemann, H. B. *et al.* The abundances of constituents of Titan's atmosphere from the GCMS instrument on the Huygens probe. *Nature* **438**, 1–6 (2005).
9. McKay, C. P., Pollack, J. B. & Courtin, R. The thermal structure of Titan's atmosphere. *Icarus* **80**, 23–53 (1989).
10. Mellor, G. L. & Yamada, T. Development of a turbulent closure model for geophysical fluid problems. *Rev. Geophys. Space Phys.* **20**, 851–875 (1982).
11. Hourdin, F., Couvreux, F. & Menut, L. Parameterization of the dry convective boundary layer based on a mass flux representation of thermals. *J. of Atm. Sci.* **59**, 1105–1123 (2002).

12. McKay, C. P., Pollack, J. B. & Courtin, R. The greenhouse and antigreenhouse effects on Titan. *Science* **253**, 1118–1121 (1991).
13. Tokano, T. The dynamics of Titan's troposphere. *Phil. Trans. R. Soc. A* **367**, 633–648 (2009).
14. Bordoni, S. & Schneider, T. Monsoons as eddy-mediated regime transitions of the tropical overturning circulation. *Nature Geoscience* **1**, 515–519 (2008).